Journal of Non-Newtonian Fluid Mechanics 250 (2017) 1–7

Contents lists available at ScienceDirect

Journal of Non-Newtonian Fluid Mechanics

journal homepage: www.elsevier.com/locate/jnnfm

Short Communication

On Poiseuille flows of a Bingham plastic with pressure-dependent rheological parameters

Yiolanda Damianou, Georgios C. Georgiou*

Department of Mathematics and Statistics, University of Cyprus, P.O. Box 20537, Nicosia 1678 Cyprus

ARTICLE INFO

Keywords:
Bingham plastic
Poiseuille flow
Pressure-dependent viscosity
Pressure-dependent yield stress

ABSTRACT

The plane Poiseuille flow of a Bingham plastic with pressure-dependent material parameters is analysed. Both the plastic viscosity and the yield stress are assumed to vary linearly with pressure and analytical solutions are derived for the two-dimensional pressure and the one-dimensional velocity. The effects of the plastic-viscosity and yield-stress growth parameters on the thickness of the unyielded plug and the conditions for the occurrence of flow are discussed.

1. Introduction

The effects of the pressure dependence of the rheological parameters of viscoplastic materials are of interest in the present work. Barus [1] proposed an exponential isothermal equation of state for the Newtonian viscosity of the form

$$\eta^*(p^*) = \eta_0^* \exp[\alpha^*(p^* - p_0^*)] \tag{1}$$

where p^* is the pressure, η_0^* is the viscosity at the reference pressure p_0^*, and α^* is the viscosity growth coefficient. Throughout this note, symbols with stars denote dimensional quantities. Other equations describing the pressure-dependence of the viscosity have also been proposed [2]. The following linear approximation of the Barus Eq. (1) at low pressures and/or for low values of the viscosity growth coefficient

$$\eta^*(p^*) = \eta_0^* [1 + \alpha^*(p^* - p_0^*)] \tag{2}$$

has also been used by various investigators (see [3] and references therein). A major difficulty with this equation is that it does not guarantee positive definiteness of the viscosity which requires the pressure to remain positive [4].

The pressure-dependence of the yield stress of viscoplastic materials (i.e., materials with yield stress τ_y^*) is well established in the mechanics of solid and granular materials [5]. Using a controlled stress rheometer combined with a double helical ribbon geometry, Hermoso et al. [6] investigated the combined effects of pressure and temperature on the rheological behaviour of two oil-based drilling fluids and found that this is described fairly well with the Bingham-plastic or the Herschel–Bulkley models. In the range of their experimental conditions, the yield stress decreased linearly with temperature and increased linearly with pressure. In order to model the isothermal yield stress behaviour of the two drilling fluids, Hermoso et al. [6] employed the following linear equation

$$\tau_y^*(p^*) = \tau_0^* [1 + \beta^*(p^* - p_0^*)] \tag{3}$$

where τ_0^* denotes the yield stress at a reference pressure p_0^* and β^* is the yield-stress growth coefficient. Hermoso et al. [6] provided tables with values of α^* and β^* at different temperatures. As an example, for the B34 fluid, which was found to follow the Bingham plastic constitutive equation, the approximate values of these two parameters at 40 °C are $\alpha^* = 2.92 \times 10^{-3}\ \text{bar}^{-1}$ and $\beta^* = 9.75 \times 10^{-3}\ \text{bar}^{-1}$ [6]. In the present work, the yield stress is allowed to decrease with pressure, i.e. β^* may be negative.

Fusi et al. [7] derived solutions of plane Poiseuille and Couette flows of a Bingham plastic and determined conditions for existence or non- existence of a rigid plug under the assumption that in the yielded region of the flow the velocity is one-dimensional while the pressure is two-dimensional. They derived explicit solutions for the case where the yield stress satisfies the linear Eq. (3) and the plastic viscosity μ^* also varies linearly and vanishes at zero relative pressure, i.e.

$$\mu^*(p^*) = \bar{\alpha}^*(p^* - p_0^*) \tag{4}$$

where the constant $\bar{\alpha}^*$ has time units. With this assumption, the derivation of an analytical solution becomes easier but the flows of a Bingham plastic with constant rheological parameters or with constant plastic viscosity are not special cases of the flow considered. This shortcoming is avoided in the present work, where the following linear expression is used instead

$$\mu^*(p^*) = \mu_0^* [1 + \alpha^*(p^* - p_0^*)] \tag{5}$$

* Corresponding author.
E-mail address: georgios@ucy.ac.cy (G.C. Georgiou).

http://dx.doi.org/10.1016/j.jnnfm.2017.10.002
Received 28 June 2017; Received in revised form 30 September 2017; Accepted 7 October 2017
Available online 12 October 2017

where μ_0^* is the plastic viscosity at a reference pressure p_0^* and $\alpha^* \geq 0$ is the corresponding growth coefficient.

2. Plane Poiseuille flow

We consider incompressible Bingham plastics with rheological parameters varying linearly with the pressure, i.e. following Eqs. (5) and (3), respectively. The tensorial form of the constitutive equation can then be written as follows [8]:

$$\begin{cases} \mathbf{D}^* = \mathbf{0}, & \tau^* \leq \tau_y^*(p^*) \\ \boldsymbol{\tau}^* = 2\left[\dfrac{\tau_0^*[1+\beta^*(p^*-p_0^*)]}{\dot{\gamma}^*} + \mu_0^*[1+\alpha^*(p^*-p_0^*)]\right]\mathbf{D}^*, & \tau^* > \tau_y^*(p^*) \end{cases} \tag{6}$$

where $\boldsymbol{\tau}^*$ is the viscous stress tensor, $\mathbf{D}^* \equiv [\nabla^*\mathbf{v}^* + (\nabla^*\mathbf{v}^*)^T]/2$ is the rate of deformation tensor, $\mathbf{v}^*$ is the velocity vector, and $\dot{\gamma}^* \equiv \sqrt{\mathrm{tr}\mathbf{D}^{*2}/2}$ and $\tau^* \equiv \sqrt{\mathrm{tr}\tau^{*2}/2}$ are the magnitudes of $\mathbf{D}^*$ and $\boldsymbol{\tau}^*$, respectively. The case of one material parameter being constant is recovered by zeroing the corresponding growth parameter. When $\alpha^* = \beta^* = 0$, Eq. (6) is reduced to the classical Bingham plastic constitutive equation with constant material parameters. Setting $\tau_0^* = 0$, Eq. (6) degenerates to the Newtonian constitutive equation with pressure-dependent viscosity.

Consider now the Poiseuille flow of a material obeying Eq. (6) in a horizontal channel of constant semi-width H^* and length L^*, as illustrated in Fig. 1. The x- and y-axes are taken in the main-flow and transverse directions, respectively and we work only in the upper part of the domain, due to symmetry. With the assumption that the flow is unidirectional with $u_x^* = u_x^*(y^*)$ and $u_y^* = 0$, the unyielded region, i.e. the region where the first branch of the constitutive Eq. (6) applies and the material moves as a plug, is defined by the yield surface $y^* = \sigma^*$, where $0 < \sigma^* < H^*$ (see Fig. 1).

In the yielded region where the second branch of the constitutive equation applies, i.e. for $(x^*, y^*) \in [0, L^*] \times [\sigma^*, H^*]$, the pressure is two-dimensional: $p^* = p^*(x^*, y^*)$. It turns out that the only non-zero component of the stress tensor is the shear stress:

$$\tau_{yx}^* = -\tau_0^*[1+\beta^*(p^*-p_0^*)] + \mu_0^*[1+\alpha^*(p^*-p_0^*)]\frac{du_x^*}{dy^*} \tag{7}$$

In the unyielded region, i.e. for $(x^*, y^*) \in [0, L^*] \times [0, \sigma^*]$, the velocity is constant, i.e. $u_x^*(y^*) = u_c^*$ where u_c^* is the velocity of the plug core, and the pressure is one-dimensional: $p^*(x^*, y^*) = p^*(x^*, \sigma^*)$. Without loss of generality, we assume that

$$p^*(0, y^*) = p_i^*, \quad p^*(L^*, y^*) = p_0^*, \quad y^* \in [0, \sigma^*] \tag{8}$$

For steady-state flow in the absence of body forces, the integral balance of linear momentum in the unyielded region gives [9]:

$$\int_0^{L^*} \tau_{yx}^*|_{y^*=\sigma^*} dx^* + \sigma^*(p_i^* - p_0^*) = 0 \tag{9}$$

Given that at the yield surface ($y^* = \sigma^*$) the velocity derivative vanishes, from Eqs. (7) and (9) we find that

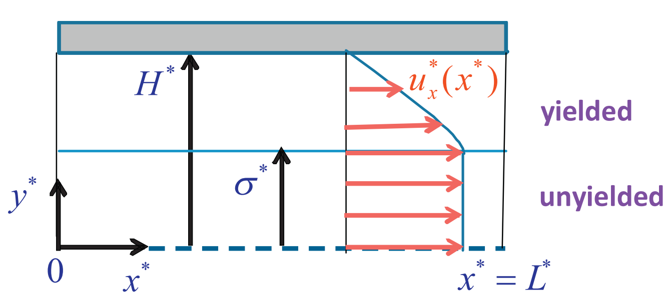

Fig. 1. Geometry of the flow and sketch of the velocity profile.

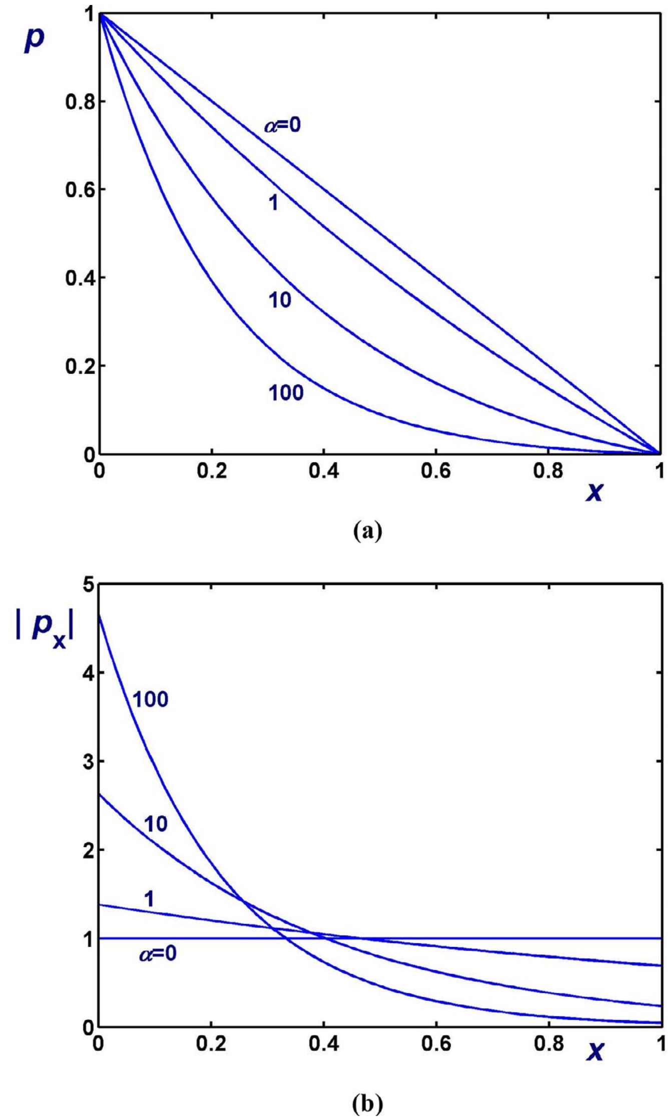

Fig. 2. Dimensionless pressure (a) and pressure-gradient (b) distributions in the unyielded core (where the pressure is one-dimensional) for various values of the plastic-viscosity growth parameter α. These results are independent of the Bingham number and the yield-stress growth number, which however affect the semi-width of the plug.

$$\sigma^* = \left[1 + \frac{\beta^*}{L^*}\int_0^{L^*}(p^* - p_0^*)dx^*\right]\frac{\tau_0^* L^*}{\Delta p^*} \tag{10}$$

where $\Delta p^* \equiv p_i^* - p_0^*$. (Recall that the pressure is one-dimensional in the unyielded region.) The above expression is valid provided that $\sigma^* < H^*$ for otherwise there is no flow due to the no-slip condition at the wall. Since the plastic-viscosity growth parameter α^* affects the pressure p^*, σ^* depends on both α^* and β^*. When $\beta^* = 0$, however, the yield point is independent of α^*.

2.1. Non-dimensionalisation

The problem is dedimensionalised by scaling x^* by L^*, y^*, h^*, and σ^* by H^*, $(p^* - p_0^*)$ by Δp^*, u_x^* by $\Delta p^* H^{*2}/(\mu_0^* L^*)$, and the stress components by $\Delta p^* H^*/L^*$. The dimensionless form of Eq. (10) becomes

$$\sigma = \left(1 + \beta\int_0^1 p\,dx\right)Bn \tag{11}$$

where $0 < \sigma < 1$, $Bn \equiv \tau_0^* L^*/(\Delta p^* H^*)$ is the Bingham number and $\beta \equiv \beta^*\Delta p^*$ is the dimensionless yield-stress growth coefficient.

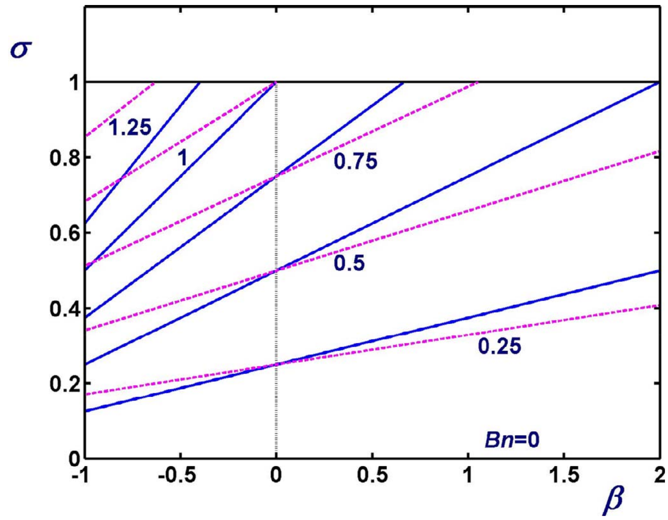

Fig. 3. Variation of the yield point with the yield-stress growth number β for $\alpha = 0$ (solid lines, constant plastic viscosity) and $\alpha = 10$ (dashed lines) and various values of the Bingham number.

It is clear that when $\sigma = 1$, there is no flow, since the unyielded core touches the wall at which no-slip applies. The critical Bingham number at which there is no flow,

$$Bn_c = \frac{1}{1 + \beta \int_0^1 p dx} \tag{12}$$

is obviously inversely proportional to the lowest dimensional pressure difference above which yielding occurs ($\Delta p_c^* = \tau_0^* L^*/(H^* Bn_c)$).

In the yielded region, i.e. for $(x, y) \in [0, 1] \times [\sigma, 1]$, the dimensionless shear stress is given by

$$\tau_{yx} = -Bn(1 + \beta p) + (1 + \alpha p)\frac{du_x}{dy} \tag{13}$$

where $\alpha \equiv \alpha^* \Delta p^*$ is the plastic-viscosity growth coefficient. The continuity equation is automatically satisfied and the two components of the momentum equation read:

$$-\frac{\partial p}{\partial x} + \frac{\partial \tau_{yx}}{\partial y} = 0 \tag{14}$$

and

$$-\frac{\partial p}{\partial y} + \varepsilon^2 \frac{\partial \tau_{yx}}{\partial x} = 0 \tag{15}$$

where $\varepsilon \equiv H^*/L^*$ is the channel aspect ratio.

Substituting Eq. (13) into Eqs. (14) and (15) we get

$$\frac{\partial p}{\partial x} = \left(\alpha \frac{du_x}{dy} - Bn\beta\right)\frac{\partial p}{\partial y} + (1 + \alpha p)\frac{d^2 u_x}{dy^2} \tag{16}$$

and

$$\frac{\partial p}{\partial y} = \varepsilon^2 \left(\alpha \frac{du_x}{dy} - Bn\beta\right)\frac{\partial p}{\partial x} \tag{17}$$

Substituting Eq. (17) into Eq. (16) and separating variables we obtain:

$$\frac{\partial p/\partial x}{1 + \alpha p} = \frac{d^2 u_x/dy^2}{1 - \varepsilon^2(\alpha du_x/dy - Bn\beta)^2} = -\Lambda \tag{18}$$

where Λ is a constant to be determined. Solving the resulting ordinary differential equation for v_x and applying the boundary conditions $du_x/dy(\sigma) = u_x(1) = 0$, one gets:

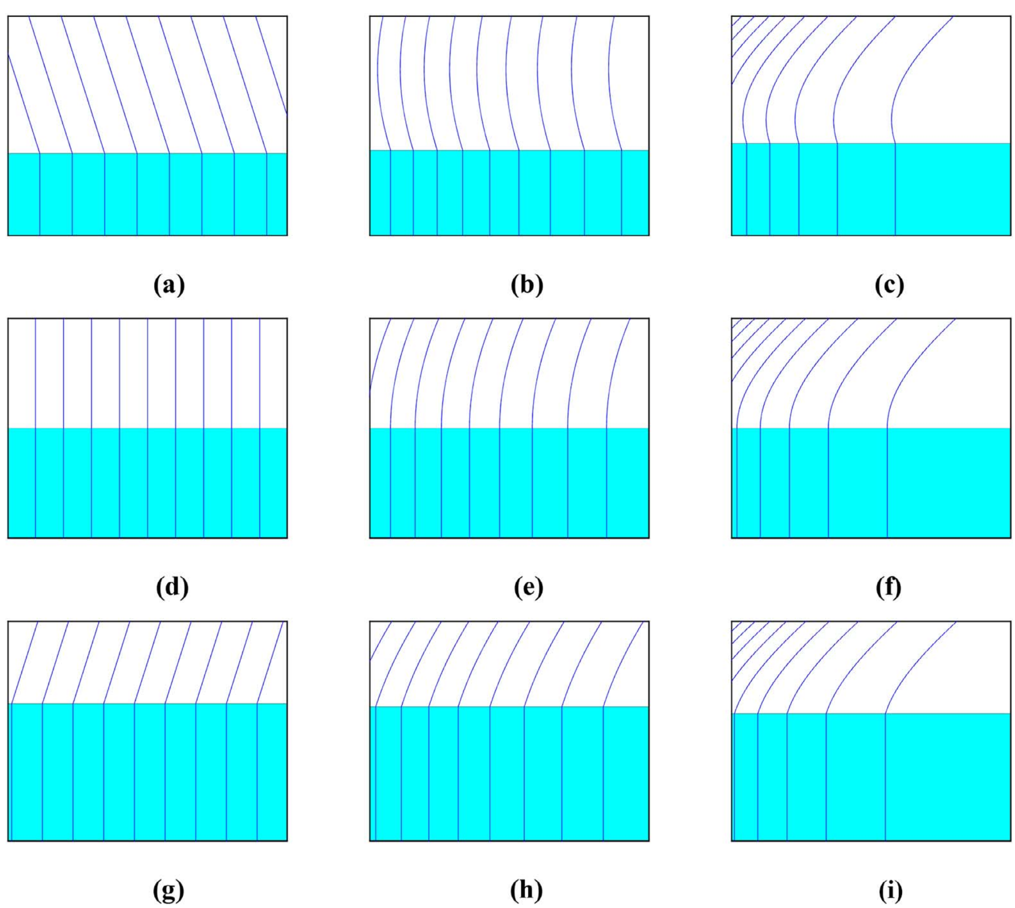

Fig. 4. Effect of the plastic-viscosity and yield stress growth parameters α and β on the pressure for $Bn = 0.5$ and $\varepsilon = 1$: (a) $\alpha = 0$, $\beta = -0.5$; (b) $\alpha = 1$, $\beta = -0.5$; (c) $\alpha = 10$, $\beta = -0.5$; (d) $\alpha = 0$, $\beta = 0$; (e) $\alpha = 1$, $\beta = 0$; (f) $\alpha = 10$, $\beta = 0$; (g) $\alpha = 0$, $\beta = 0.5$; (h) $\alpha = 1$, $\beta = 0.5$; (i) $\alpha = 10$, $\beta = 0.5$. As α is increased, the thickness of the unyielded plug increases if $\beta < 0$ (first row), remains constant if $\beta = 0$ (middle row), and increases if $\beta > 0$ (third row). The high value of ε was chosen in order to exaggerate the differences.

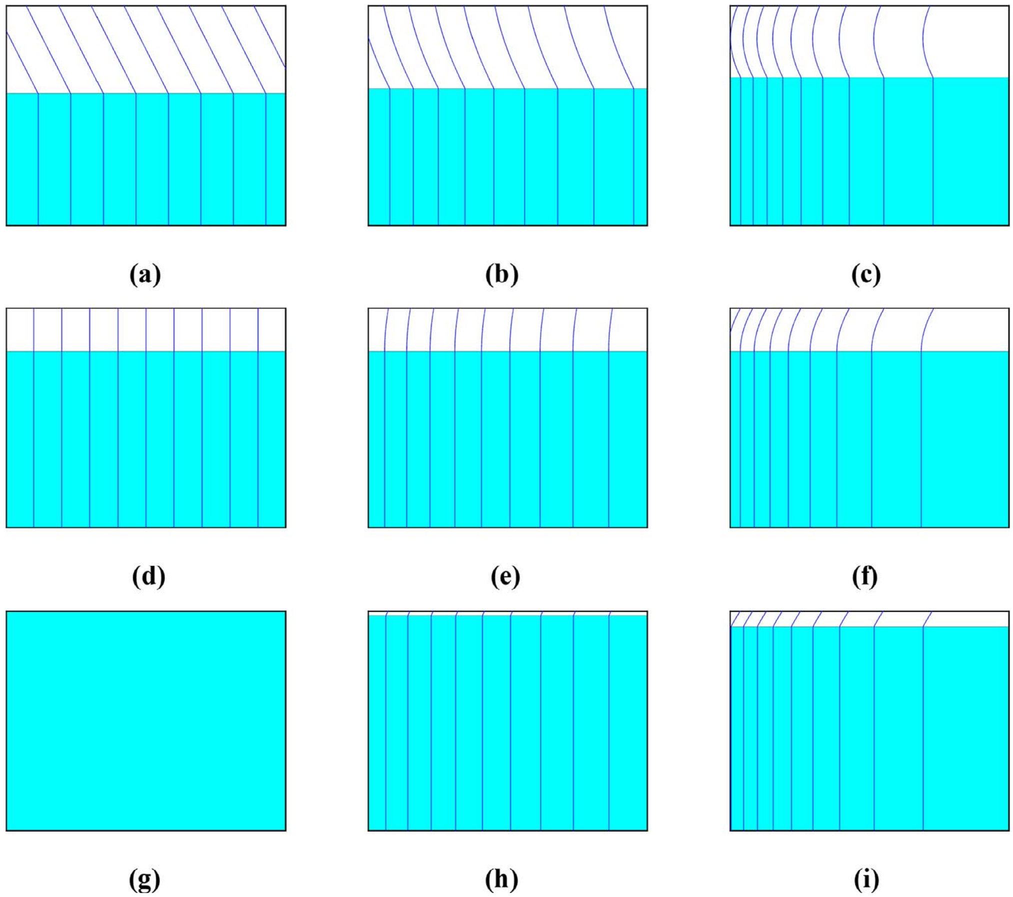

Fig. 5. Effect of the plastic-viscosity and yield stress growth parameters α and β on the pressure for $Bn = 0.8$ and $\varepsilon = 1$: (a) $\alpha = 0$, $\beta = -0.5$; (b) $\alpha = 1$, $\beta = -0.5$; (c) $\alpha = 10$, $\beta = -0.5$; (d) $\alpha = 0$, $\beta = 0$; (e) $\alpha = 1$, $\beta = 0$; (f) $\alpha = 10$, $\beta = 0$; (g) $\alpha = 0$, $\beta = 0.5$ ($Bn = Bn_c$ in this case); (h) $\alpha = 1$, $\beta = 0.5$; (i) $\alpha = 10$, $\beta = 0.5$. The high value of ε was chosen in order to exaggerate the differences.

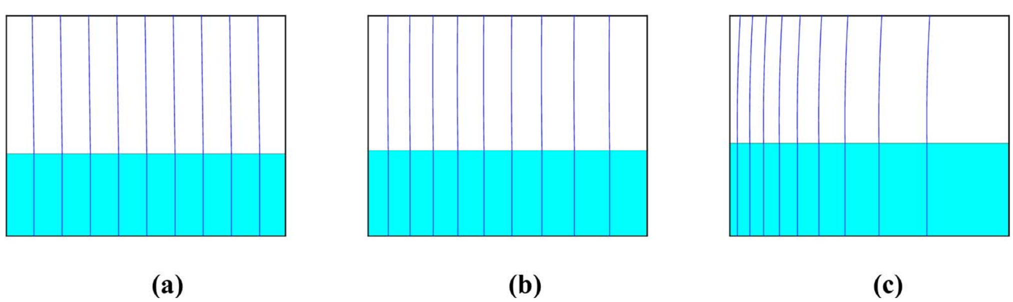

Fig. 6. Effect of the plastic-viscosity and yield stress growth parameters α and β on the pressure for $\beta = -0.5$, $Bn = 0.5$ and $\varepsilon = 0.2$: (a) $\alpha = 0$; (b) $\alpha = 1$; (c) $\alpha = 10$. The counterparts of these results for $\varepsilon = 1$ are those in the first row of Fig. 3.

$$u_x(y) = \frac{1}{\varepsilon^2\alpha^2\Lambda}\log\frac{\cosh[\varepsilon\alpha\Lambda(1-\sigma)+\tanh^{-1}(\varepsilon Bn\beta)]}{\cosh[\varepsilon\alpha\Lambda(y-\sigma)+\tanh^{-1}(\varepsilon Bn\beta)]} - \frac{Bn\beta}{\alpha}(1-y), \quad \sigma \le y \le 1 \tag{19}$$

where $\alpha > 0$. (The case $\alpha = 0$ will be considered below.) Integrating now the ordinary differential equation for the pressure in Eq. (18) yields

$$p(x, y) = \frac{1}{\alpha}[w(y)e^{-\alpha\Lambda x} - 1], \quad \sigma \le y \le 1 \tag{20}$$

where $w(y)$ is an unknown function. Substituting p and u_x into Eq. (17), we get a first order differential equation for w,

$$w'(y) + \varepsilon\alpha\Lambda\tanh[\varepsilon\alpha\Lambda(y-\sigma)+\tanh^{-1}(\varepsilon Bn\beta)]w(y) = 0 \tag{21}$$

the solution of which is

$$w(y) = C\cosh[\varepsilon\alpha\Lambda(y-\sigma)+\tanh^{-1}(\varepsilon Bn\beta)] \tag{22}$$

where C is an integration constant. Applying the conditions $p(0, \sigma) = 1$ and $p(1, \sigma) = 0$ we find

$$C = \frac{1+\alpha}{\cosh[\tanh^{-1}(\varepsilon Bn\beta)]} \quad \text{and} \quad \Lambda = \frac{\ln(1+\alpha)}{\alpha}$$

Therefore, we have:

$$p(x, y) = \begin{cases} \frac{1}{\alpha}\left[(1+\alpha)^{1-x\frac{\cosh[\varepsilon\ln(1+\alpha)(y-\sigma)+\tanh^{-1}(\varepsilon Bn\beta)]}{\cosh[\tanh^{-1}(\varepsilon Bn\beta)]}} - 1\right], & \sigma \le y \le 1 \\ \frac{1}{\alpha}[(1+\alpha)^{1-x} - 1], & 0 \le y < \sigma \end{cases} \tag{23}$$

As for the velocity, we find

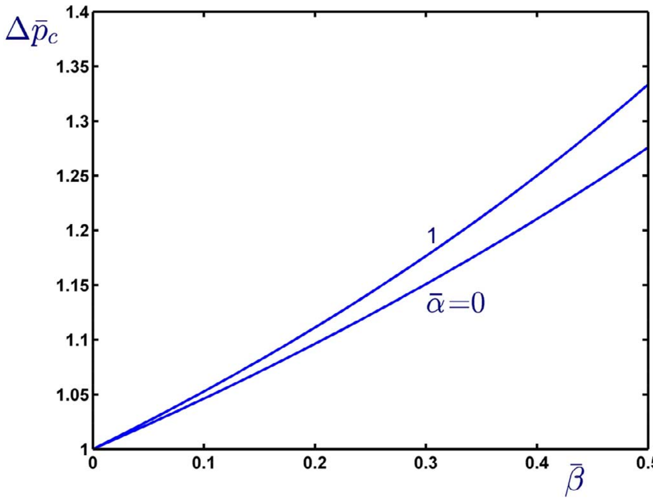

Fig. 7. Variation of the critical pressure difference $\Delta\bar{p}_c \equiv \Delta p_c^*/(\tau_0^* L^*/H^*)$ required for the initiation of Bingham-plastic flow with the yield-stress growth parameter $\bar{\beta}$ for $\bar{\alpha}=0$ and 1.

$$u_x(y)=\begin{cases}\dfrac{1}{\alpha\varepsilon^2\ln(1+\alpha)}\ln\dfrac{\cosh[\varepsilon\ln(1+\alpha)(1-\sigma)+\tanh^{-1}(\varepsilon Bn\beta)]}{\cosh[\varepsilon\ln(1+\alpha)(y-\sigma)+\tanh^{-1}(\varepsilon Bn\beta)]}-\dfrac{Bn\beta}{\alpha}(1-y), & \sigma\le y\le 1\\[2ex] \dfrac{1}{\alpha\varepsilon^2\ln(1+\alpha)}\ln\dfrac{\cosh[\varepsilon\ln(1+\alpha)(1-\sigma)+\tanh^{-1}(\varepsilon Bn\beta)]}{\cosh[\tanh^{-1}(\varepsilon Bn\beta)]}-\dfrac{Bn\beta}{\alpha}(1-\sigma), & 0\le y<\sigma\end{cases} \tag{24}$$

By means of Eq. (11), the yield point is given by

$$\sigma=\left\{1+\left[\frac{1}{\ln(\alpha+1)}-\frac{1}{\alpha}\right]\beta\right\}Bn \tag{25}$$

Flow occurs provided that $\sigma<1$, i.e. when the Bingham number is lower than the critical value

$$Bn_c=\frac{1}{1+\left[\frac{1}{\ln(\alpha+1)}-\frac{1}{\alpha}\right]\beta} \tag{26}$$

If now Bn is specified, then the maximum value of β at which there is flow is

$$\beta_c\equiv\frac{1/Bn-1}{\frac{1}{\ln(\alpha+1)}-\frac{1}{\alpha}} \tag{27}$$

Recall that the Bingham number is inversely proportional to the lowest dimensional pressure difference above which yielding occurs. Note that β may be negative in which case the yield stress is decreasing downstream and thus Bn_cmay be greater than unity. If $\beta=0$, then $Bn_c=1$ and $\sigma=Bn$, i.e. σ is independent of the plastic-viscosity growth parameter α (this is due to the fact that the pressure is scaled by the inlet pressure Δp^*). The above solution is valid provided that $\sigma\ge 0$, i.e.

$$\beta\ge\frac{1}{\frac{1}{\alpha}-\frac{1}{\ln(\alpha+1)}} \tag{28}$$

so that the plug is not broken. As already mentioned, β may be negative and, more specifically, $\beta\ge -1$, which ensures that condition (28) is satisfied.

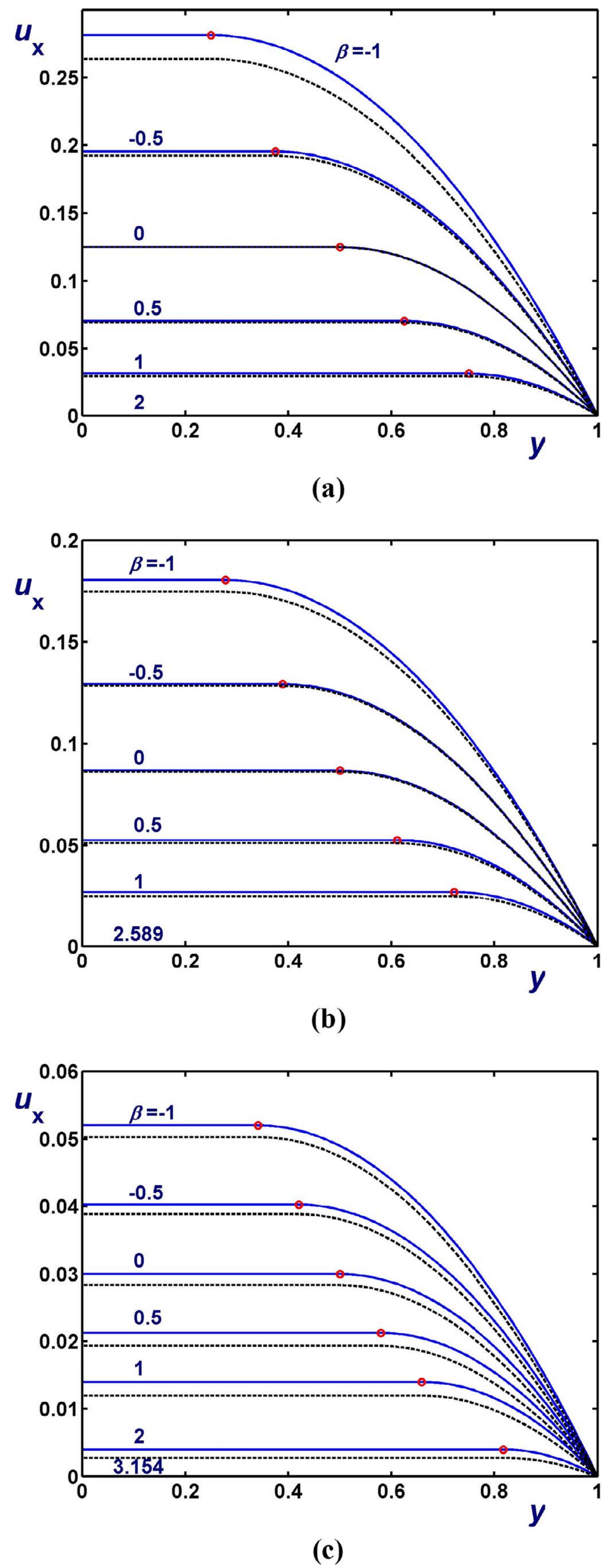

Fig. 8. Velocity distributions of Bingham plastic flow for $Bn=0.5$, $\varepsilon=0$ (solid) and $\varepsilon=0.5$ (dashed), and various values of the yield-stress-growth parameter ranging from $\beta=-1$ (lower bound) to β_c (no flow): (a) $\alpha=0$ (constant viscosity); (b) $\alpha=1$; (c) $\alpha=10$. The circles show the positions of the yield point.

The above analytical solution yields the classical constant-parameter Bingham solution by setting $\alpha = \beta = 0$. The special solutions for $\alpha = 0$ and $\beta = 0$ are summarized below.

2.2. Constant plastic viscosity ($\alpha = 0$)

In the case of constant plastic viscosity, Eq. (18) becomes

$$\frac{\partial p}{\partial x} = \frac{d^2u_x/dy^2}{1-\varepsilon^2(\alpha du_x/dy - Bn\beta)^2} = -\Lambda \tag{29}$$

It is easily shown that

$$u_x(y) = \begin{cases} \frac{1}{2}(1-\varepsilon^2 Bn^2\beta^2)(1+y-2\sigma)(1-y), & \sigma \le y \le 1 \\ \frac{1}{2}(1-\varepsilon^2 Bn^2\beta^2)(1-\sigma)^2, & 0 \le y < \sigma \end{cases} \tag{30}$$

and

$$p(x,y) = \begin{cases} \varepsilon^2 Bn\beta(y-\sigma) + 1 - x, & \sigma \le y \le 1 \\ 1-x, & 0 \le y < \sigma \end{cases} \tag{31}$$

where

$$\sigma = (1+\beta/2)Bn \tag{32}$$

The critical Bingham number above which there is no flow is:

$$Bn_c = \frac{1}{1+\beta/2} \tag{33}$$

where $\beta > -2$. Setting $\beta = 0$ gives the solution of a Bingham plastic with constant rheological parameters and setting $Bn = 0$ yields $\sigma = 0$ and the Newtonian solution. For β_c we find

$$\beta_c = 2\left(\frac{1}{Bn} - 1\right) \tag{34}$$

2.3. Constant yield stress ($\beta = 0$)

In the case of a Bingham plastic with constant yield stress ($\beta = 0$), the solution is simplified as follows:

$$u_x(y) = \frac{1}{\alpha\varepsilon^2\ln(1+\alpha)} \begin{cases} \ln\dfrac{\cosh[\varepsilon\ln(1+\alpha)(1-\sigma)]}{\cosh[\varepsilon\ln(1+\alpha)(y-\sigma)]}, & \sigma \le y \le 1 \\ \ln(\cosh[\varepsilon\ln(1+\alpha)(1-\sigma)]), & 0 \le y < \sigma \end{cases} \tag{35}$$

and

$$p(x,y) = \begin{cases} \dfrac{1}{\alpha}[(1+\alpha)^{1-x}\cosh\{\varepsilon\ln(1+\alpha)(y-\sigma)\} - 1], & \sigma \le y \le 1 \\ \dfrac{1}{\alpha}[(1+\alpha)^{1-x} - 1], & 0 \le y < \sigma \end{cases} \tag{36}$$

where $\sigma = Bn$. Setting $\sigma = Bn = 0$ yields the solution of a Newtonian fluid with a pressure-dependent velocity [3].

3. Pressure distributions and velocity profiles

As already mentioned, in the plug the pressure is one-dimensional, i.e. $p = p(x)$. From Eq. (23) it is deduced that the pressure distribution in the unyielded region is independent of the Bingham number and the yield-stress growth number, which however affect the semi-width σ of the unyielded core. The effect of the viscosity growth parameter is illustrated in Fig. 2, where both the pressure p and its derivative $|p_x|$ are plotted for various values of α. As α is increased the required pressure gradient grows higher at the inlet plane where the viscosity attains its maximum value and reduces more rapidly upstream and more slowly downstream.

The effect of the various parameters on the yield point is illustrated in Fig. 3, where σ is plotted versus β for $\alpha = 0$ (solid lines) and $\alpha = 10$ (dashed lines) and various values of the Bingham number. We observe that when $\beta > 0$ the yield point moves towards the midplane as α is increased and that this trend is reversed when $\beta < 0$. It is also clear that for a given value of the yield-stress growth number β, the yield point increases as the Bingham number is increased up to the corresponding critical Bingham number Bn_c and that the range of admissible Bingham numbers is wider when β is negative, i.e. when the yield stress decreases with pressure. The critical Bingham number increases with α when $\beta > 0$ and decreases when $\beta < 0$. On the other hand, for a given Bingham number there is a critical value of β at which $\sigma = 1$ and there is no flow.

In the yielded region, the pressure is two-dimensional. The effects of the growth parameters α and β on the pressure contours as well as on the semi-width of the plug are illustrated in Fig. 4 for $Bn = 0.5$ and $\varepsilon = 1$. The latter value was intentionally taken to be high, in order to make the changes in the solution more visible. It can be seen that, depending on whether $\beta < 0$ (first row), $\beta = 0$ (second row), or $\beta > 0$ (third row), σ increases, remains constant, or decreases with α, respectively. Irrespective of the values of α and Bn, σ increases with the yield-stress growth parameter β. Figure 5 shows similar results for a higher Bingham number, i.e. $Bn = 0.8$. The main difference from the results for $Bn = 0.5$ in Fig. 4 is that σ is higher in all cases. In particular, when $\alpha = 0$ and $\beta = 0.5$ (Fig. 5g) there is no flow, i.e. $\sigma = 1$; from Eq. (33), $Bn_c = 1/(1+\beta/2) = 0.8$. The effect of ε is illustrated in Fig. 5, which shows the counterparts of Fig. 4a–c (first row) when ε is smaller ($\varepsilon = 0.2$ instead of $\varepsilon = 1$). The bending of the pressure contours in the yielded region is not so pronounced despite the fact that the value of ε is still high.

Calculating the critical pressure difference required to start the flow is of importance in engineering applications. Switching to new non-dimensionalization scales one finds from Eq. (26) that

$$\Delta\bar{p}_c[1 - \bar{\beta}/\ln(1+\bar{\alpha}\,\Delta\bar{p}_c)] + \frac{\bar{\beta}}{\bar{\alpha}} - 1 = 0 \tag{37}$$

where the bars denote the new dimensionless variables, the pressure is now scaled by $\tau_0^* L^*/H^*$, $\bar{\alpha} \equiv \alpha^*\tau_0^* L^*/H^*$ and $\bar{\beta} \equiv \beta^*\tau_0^* L^*/H^*$. When $\bar{\alpha} = 0$ it is easily found that

$$\Delta\bar{p}_c = \frac{1}{1-\bar{\beta}/2} \tag{38}$$

The effect of the new dimensionless viscosity and yield-stress growth numbers, $\bar{\alpha}$ and $\bar{\beta}$, on the critical pressure difference is illustrated in Fig. 7. As expected, $\Delta\bar{p}_c$ increases with both parameters, with the dependence on $\bar{\beta}$ being stronger. The effect of $\bar{\alpha}$ is enhanced as $\bar{\beta}$ is increased.

Finally, Fig. 8 shows representative velocity profiles of a Bingham plastic with $Bn = 0.5$, $\varepsilon = 0$ (solid) and $\varepsilon = 0.5$ (dashed), and various values of β for three values of the plastic-viscosity parameter, i.e. $\alpha = 0$ (constant viscosity), 1, and 10, which actually correspond to the middle row of Fig. 3. The velocity profiles for $\varepsilon = 0$ have been obtained using the first term of the Taylor-series expansion of $u_x(y)$ in Eq. (24) in terms of ε:

$$u_x(y) = \frac{\ln(1+\alpha)}{2\alpha} \begin{cases} (1+y-\sigma)(1-y), & \sigma \le y \le 1 \\ (1-\sigma)^2, & 0 \le y < \sigma \end{cases} + O(\varepsilon^2) \tag{39}$$

Note that the velocity is reduced as α is increased. Since the Bingham number is specified, there is an upper bound for the admissible values of β which corresponds to the value at which $\sigma = 1$ (no flow). From Eqs. (27) and (34) we find that $\beta_c = 2$, 2.589 and 3.154 for $\alpha = 0$, 1, and 10, respectively. The velocity profiles of Fig. 8 correspond to different values of β in the range $(-1, \beta_c)$. As β is increased the velocity is reduced and the yield point tends to and eventually reaches the wall when $\beta = \beta_c$.

References

[1] C. Barus, Isothermals, isopiestics and isometrics relative to viscosity, Amer. J. Sci. 45 (1893) 87–96.
[2] J. Málek, K.R. Rajagopal, Mathematical properties of the solutions to the equations governing the flow of fluids with pressure and shear rate dependent viscosities, Handbook of Mathematical Fluid Dynamics, Elsevier, 2007.
[3] A. Kalogirou, S. Poyiadji, G.C. Georgiou, Incompressible Poiseuille flows of Newtonian liquids with a pressure/dependent viscosity, J. Non-Newtonian Fluid Mech. 166 (2011) 413–419.
[4] S.A. Suslov, T.D. Tran, Revisiting plane Couette-Poiseuille flows of piezo-viscous fluid, J. non-Newtonian Fluid Mech. 154 (2008) 170–178.
[5] I.R. Ionescu, A. Mangeney, F. Bouchut, O. Roche, Viscoplastic modeling of granular column collapse with pressure-dependent rheology, J. Non-Newtonian Fluid Mech. 219 (2015) 1–18.
[6] J. Hermoso, F. Martinez-Boza, C. Gallegos, Combined effect of pressure and temperature on the viscous behaviour of all-oil drilling fluids, Oil Gas Sci. Technol. – Rev. IFP Energies Nouvelles 69 (2014) 1283–1296.
[7] L. Fusi, A. Farina, F. Rosso, Bingham flows with pressure-dependent rheological parameters, Int. J. Nonlinear Mech. 64 (2014) 33–38.
[8] EC Bingham, Fluidity and Plasticity, McGraw Hill, New-York, 1922.
[9] L. Fusi, A. Farina, F. Ross, S. Roscani, Pressure-driven lubrication flow of a Bingham fluid in a channel: a novel approach, J. Non-Newtonian Fluid Mech. 221 (2015) 66–75.